



A novel method for predicting decomposition onset temperature of high-energy metal–organic frameworks

Amir Rajaei¹ · Mohammad Jafari¹ · Kamal Ghani¹

Received: 22 July 2019 / Accepted: 29 December 2019 / Published online: 9 January 2020
© Akadémiai Kiadó, Budapest, Hungary 2020

Abstract

The decomposition onset temperature, T_{decom} , is an important parameter for investigating the thermal stability of chemicals. A novel method is introduced for the prediction of T_{decom} of metal–organic frameworks, MOFs, through their structural parameters. It can be applied for different kinds of MOFs containing different secondary building units, SBUs. The new model is based on the coordination number of metal atoms in the SBU, and some structural moieties that depend on the type, number, and bond strength of organic and inorganic substituents. The present model is easily applicable for MOFs containing complex SBUs, without using complicated computer codes. Coefficient of determination, R^2 , for new model is 0.9124, and reliability of model is confirmed with statistical parameters such as root-mean-squared error, RMSE, mean absolute percent error, MAPE, and maximum of errors, which are 28.1, 7.3, and 74.9 °C, respectively. Further eight MOFs including complex SBUs are tested with this method which gives good results. In order to evaluate goodness of fit, goodness of prediction, accuracy, and precision of the new model, cross-validation is done.

Keywords Decomposition onset temperature · MOF · Molecular structure · Thermal stability · SBU

Introduction

Metal–organic frameworks, MOFs, known as a class of porous compounds, consist of metal centers and organic components, called node and linker, respectively. The metal centers can be in ionic or cluster forms. Study of several synthesized MOFs shows that the metal centers are usually in cluster form rather than single atom [1]. Widely used metal ions in MOFs are two, three, and four valence cations such as Cu^{2+} , Zn^{2+} , Co^{2+} , Fe^{3+} , and Zr^{4+} which can create different coordination geometries; square, tetrahedral, octahedral, trigonal, and pyramidal. Carboxylates, amines, phosphates, and sulfonates are the most popular organic linkers that use in MOFs. Inorganic and organic units are linked by coordination bonds to make several SBUs which have been identified as a useful tool in the analysis of complex MOFs [2].

MOFs have several applications in many scientific fields, due to their unique structures. They have been applied for catalytic purpose, separation, gas storage, biomedical applications, luminescence, magnetism, proton conduction, and chemical sensing [1, 3–7].

There are several studies about specific properties of MOFs, such as their mechanical, chemical, and thermal stability. Theoretical and experimental works show the importance of thermal stability of MOFs for several applications such as gas storage and catalysis [8–14]. For example, the thermal stability of Pd/MIXMOF catalyst in the oxidation of CO in 225 °C is an important factor [15]. As another example, in the hydrogen sorption by the ZIF-8, evacuation of MOF has been done at the 300 °C, so the thermal stability of ZIF-8 is an important parameter [16].

Thermal stability of MOFs is related to node–linker bond breakage, usually. Owing to this, the strength of node–linker bond and the number of linkers connected to metal node are effective parameters in thermal behavior of MOFs [17]. Since MOFs constructed from strong bonds, e.g., M–O, M–N, C–O, and C–C, they usually have high thermal stability from 250 to 500 °C [5, 16, 18, 19].

A proper method for determination of thermal stability of MOFs is thermogravimetric analysis, TGA [17]. Based on

✉ Mohammad Jafari
jafariememzadeh@gmail.com

✉ Kamal Ghani
kghani@mut-es.ac.ir

¹ Department of Chemistry, Malek-ashtar University of Technology, Shahin-Shahr, P.O. Box 83145/115, Islamic Republic of Iran

TGA results, decomposition of MOFs occurs in three steps. At first step, separation of uncoordinated guest molecules, usually solvent molecules, occurs. In this step, MOF configuration is still stable and efficient. Coordinated molecules, usually node–linker bonds, separate in second step. It means that MOF configuration is not stable anymore. And finally, full decomposition of MOF occurs. Since destruction of MOF starts from second step, the thermal stability of MOF depends on node–linker bond breakage [13].

Development and spread of theoretical methods can help scientists to predict thermal stabilities of MOFs and choosing suitable MOFs for any purpose. Mu et al. estimate the heat capacity contributions of organic functional groups using the group contribution method. They examined thermal stability of several MOFs with different coordination numbers and topologies such as IRMOF-1(ZnBDC), MOF-177(ZnBTB), UMCM-1(ZnBTB + BDC), HKUST-1 (CuBTC), and CuBTB. Among these MOFs, the thermal stabilities of HKUST-1 and CuBTB are the same, around 300 °C, and they have the same coordination numbers (CN = 6) but different topologies. Since three MOFs, UMCM-1, MOF-177, and IRMOF-1, have the same coordination numbers (CN = 4), they possess the same thermal stabilities, around 460 °C; however, they have different ligands and also different topologies [12].

Using achieved results, they showed that the thermal stability of MOFs is related to local coordination environment and coordination number rather than framework topology.

Several *in vitro*, *in vivo*, or *in silico* methods are used for estimation of physicochemical properties of substances in which quantitative structure–property relationships, QSPRs, are one of the *in silico* methods. Some other useful methods are quantitative structure–toxicity relationship, QSTR, and quantitative structure–pharmacokinetic relationship, QSPkR.

Since QSPRs are comprehensive and efficient methods, they are widely used for estimation of physicochemical properties of substances, but they ordinarily need some additional complex information, e.g., molecular descriptors and computer codes. Moreover, such complex methods require expert users [20].

Multiple linear regression, MLR, methods are simple statistical tools that make good correlation between structural property and descriptors. Several works on the development of QSPR models for regulatory frameworks [21], prediction of the onset temperature of decomposition of lubricant additives [22], a new method for assessment of glass transition temperature of ionic liquids from structure of their cations and anions without using any computer codes [23], and a novel method for predicting decomposition onset temperature of cubic polyhedral oligomeric silsesquioxane derivatives [24], have been done using this method. Fayet et al. *for example*, used constitutional and topological descriptors

to predict the heat of decomposition of nitroaromatic compounds. The correlation and internal validation were used to exhibit high performance of models. R^2 were 0.84 and 0.78 and Q_{LOO}^2 were 0.79 and 0.71, for two models, respectively. As a good example, experimental and predicted heats of decomposition for 3-nitroanisole were 243 and 247 kJ/mol, respectively [21]. In other words, the onset temperature of decomposition of lubricant additives was predicted by MLR method. Several molecular descriptors such as the presence or absence of N–S or N–O at topological distances were used to construct the model. The accuracy of their new model was proved by some statistical parameters such as, R^2 , P value, and Q_{LOO}^2 , which are 0.935, < 0.05, and 0.919, respectively. For hexyl 2-(ethoxycarbonothioylthio) acetate, experimental and predicted values of onset temperature were 245.57 and 246.27 °C, respectively [22].

Since several structural parameters of MOFs, such as number of some atoms, presence of some metals and ligands, also coordination number, described in Eq. 1 and Table 2, can be used to survey their thermal stabilities, the purpose of this paper is to construct a new simple predictive method for estimation of the decomposition onset temperature, T_{decom} , as an important parameter for the evaluation of thermal stability of MOFs with respect to SBU. It will be showed that there is no need for the complex codes and descriptors as well as expert users. The new model correlates T_{decom} to the structural parameters of MOFs using several simple molecular descriptors.

Materials and methods

Experimental T_{decom} values of 56 MOFs, which were collected from the literature, were used to construct the new model, Table 1.

However, R^2 is a good statistical parameter for evaluation of new models, and further validations are necessary. Robustness of new model can be validated by both internal and external data. In external validation, the available dataset divides into calibration and test subsets that are used for building and assessing model, respectively [20]. In the case that the dataset is small, the dividing of dataset may cause valuable information to be wasted. In this case, internal validation has been suggested [25]. The most usual technique of internal validation is cross-validation. In this method, a subset containing several data points or one data point is excepted from the dataset and the remaining data are used for constructing the model and the predictive ability of the model is tested by the unknown compounds [26]. Cross-validation methods can be split into leave-one-out cross-validation, LOO-CV, and k-fold cross-validation, k-fold CV, parts. For optimization of model parameters in order to survey flexibility of model,

Table 1 Comparison of predicted value for decomposition onset temperature of MOFs with experimental data

No.	SBU	Experimental $T_{\text{decom}}/^{\circ}\text{C}$	Predicted $T_{\text{decom}}/^{\circ}\text{C}$	Dev.
1	Cu ₂ (TPTC-OMe)	300.0 [13]	328.7	– 28.7
2	Cu ₂ (TPTC-OEt)	325.0 [13]	330.1	– 5.1
3	Cu ₂ (TPTC-OnPr)	340.0 [13]	331.4	8.6
4	Cu ₂ (TPTC-OnHex)	355.0 [13]	335.4	19.6
5	[Cu(atrz) ₃ (NO ₃) ₂] _n	243.0 [11]	250.1	– 7.1
6	[Cu(tztr)] _n	360.0 [30]	342.0	18.0
7	[Cu(ntz)] _n	315.0 [31]	333.5	– 18.5
8	[Cu(bta)(NH ₃) ₂ ·H ₂ O] _n	250.0 [37]	262.3	– 12.3
9	[Cu(pn)(N ₃) ₂] _n	215.7 [38]	177.0	38.7
10	[Cu ₂ (en) ₂ (N ₃) ₄] _n	201.8 [39]	179.3	22.5
11	[Cu(Htztr)] _n	355.0 [40]	353.7	1.3
12	[Cu(tzeg)(H ₂ O)] _n	350.0 [41]	307.1	42.9
13	[Cu ₄ Na(Mtta) ₅ (CH ₃ CN)] _n	384.0 [42]	327.8	56.2
14	{[Cu(tztr)]·H ₂ O} _n	325.0 [40]	342.7	– 17.7
15	[Cu(3,5-DNBA)(N ₃) ₂] _n	268.0 [43]	251.9	16.1
16	{(AG) ₂ [Cu(btm) ₂]} _n	212.5 [44]	233.8	– 21.3
17	Cu(ATZ)(ClO ₄) ₂] _n	250.0 [45]	286.6	– 36.6
18	Cu(Htztr) ₂ (H ₂ O) ₂] _n	345.0 [40]	326.6	18.4
19	[Cu(DNBT)(ATRZ) ₃] _n	323.2 [46]	351.8	– 28.6
20	[Cu(DNBTO)(ATRZ) ₂ (H ₂ O) ₂] _n	333.3 [46]	338.2	– 4.9
21	Cu ₂ (BTC) _{4/3}	285.0 [12]	332.8	– 47.8
22	[Zn(hdtz)].DMA	392.0 [8]	381.5	10.5
23	[Zn ₂ (N ₂ H ₄) ₃ (N ₂ H ₃ CO ₂) ₂].[ClO ₄] ₂ ·H ₂ O	293.0 [8]	236.9	56.1
24	Zn ₄ O(C ₁₂ H ₆ O ₄) ₃	400.0 [47]	379.1	20.9
25	[Zn(N ₂ H ₄) ₂ (N ₃) ₂] _n	200.9 [39]	213.0	– 12.1
26	[Zn(tzeg)] _n	425.0 [41]	371.6	53.4
27	Zn ₂ (DHBDC)(DMF) ₂ ·(H ₂ O) ₂	352.0 [48]	325.3	26.7
28	Zn _{1.72} Co _{0.28} (DHBDC)(DMF) _{0.1}	322.0 [48]	318.9	3.1
29	[Zn ₄ O(BDC)(BTB) _{4/3}]	460.0 [12]	415.1	44.9
30	Zr ₆ O ₄ (OH) ₄ (BDC) ₆ NH	380.0 [49]	454.9	– 74.9
31	Zr ₆ O ₄ (OH) ₄ (BDC) ₆	520.0 [50]	456.1	63.9
32	[La ₂ (C ₂ H ₄ C ₂ O ₄) ₂ (SO ₄)(H ₂ O) ₂]	500.0 [51]	500.0	0.0
33	[PR ² (C ₂ H ₄ C ₂ O ₄) ₂ (SO ₄)(H ₂ O) ₂]	500.0 [51]	500.0	0.0
34	[Nd ₂ (C ₂ H ₄ C ₂ O ₄) ₂ (SO ₄)(H ₂ O) ₂]	500.0 [51]	500.0	0.0
35	[Sm ₂ (C ₂ H ₄ C ₂ O ₄) ₂ (SO ₄)(H ₂ O) ₂]	500.0 [51]	500.0	0.0
36	(Co(NH ₂ NH ₂) ₅ (ClO ₄) ₂) _n	194.0 [11]	223.6	– 29.6
37	[Ag(atrz) _{1.5} (NO ₃) _n]	257.0 [11]	297.7	– 40.7
38	(AG) ₃ [Co(btm) ₃]	268.1 [30, 44]	277.4	– 9.3
39	[Ca ₃ K ₂ (C ₇ H ₂ O ₅) ₂].6H ₂ O	200.0 [52]	185.4	14.6
40	[Cd ₂ (HATr) ₄ (NO ₃) ₄ ·H ₂ O] _n	295.0 [39, 53]	270.4	24.6
41	[Cd(HATr) ₂ (ClO ₄) ₂] _n	304.9 [39, 53]	307.3	– 2.4
42	[Cd(en)(N ₃) ₂] _n	149.9 [39]	189.5	– 39.6
43	[Ni(N ₂ H ₄) ₅ (ClO ₄) ₂] _n	220.0 [39, 54]	223.6	– 3.6
44	[Cd(DAT) ₂ (N ₃) ₂] _n	208.0 [39, 55]	228.2	– 20.2
45	[Cd ₂ (NO ₃) ₂ Cl ₂ (HATr) ₂] _n	224.9 [39, 53]	220.7	4.1
46	[Pb(H ₂ tztr)(O)] _n	318.0 [39, 54]	350.9	– 32.9
47	[Cd(tzeg)(H ₂ O)] _n	375.0 [41]	356.0	19.0
48	[Sr(BTE)(H ₂ O) ₅] _n	350.0 [39, 56]	349.9	0.1
49	[Ba(BTE)(H ₂ O) ₅] _n	350.0 [39, 56]	349.9	0.1
50	[Cd ₂ (N ₂ H ₄) ₂ (N ₃) ₄] _n	151.0 [39, 57]	172.6	– 21.6

Table 1 (continued)

No.	SBU	Experimental $T_{\text{decom}}/^{\circ}\text{C}$	Predicted $T_{\text{decom}}/^{\circ}\text{C}$	Dev.
51	$[\text{Co}_9(\text{bta})_{10}(\text{Hbta})_2(\text{H}_2\text{O})_{10}]_n \cdot [22(\text{H}_2\text{O})]_n$	300.0 [39, 58]	285.3	14.7
52	$[\text{Co}_9(\text{bta})_{10}(\text{Hbta})_2(\text{H}_2\text{O})_{10}]_n$	253.0 [39, 58]	270.6	- 17.6
53	$[\text{CdCl}_2(\text{HATr})_2]$	282.9 [39, 53]	292.1	- 9.3
54	$[\text{Cd}_3(\text{BTB})_2(\text{DEF})_4]_n \cdot 3n\text{DEF}$	420.0 [12, 59]	-415.9	4.1
55	$[\text{La}(\text{BTB})(\text{H}_2\text{O})] \cdot 3\text{DMF}$	560.0 [12, 60]	576.5	- 16.5
56	$[\text{Ni}(\text{HBTB})(\text{bipy})] \cdot \text{guests}$	380.0 [12, 61]	424.2	- 44.2

Table 2 Values of two correction factors—increasing and decreasing factors—for prediction of T_{decom} of MOFs based on structural parameters

Increasing factor	
Structural parameters	T_{decom}^+
Azole derivatives	0.1
La	0.3
Decreasing factor	
Structural parameters	T_{decom}^-
Cu	0.6
Ca	3.8
M-N-M ^a	0.9
$\text{ML}_3^{\text{b}}(\text{CN}^{\text{c}} = 3)$	1.2
$\text{ML}_4(\text{CN} = 4)$	0.6
$\text{ML}_5(\text{CN} = 5)$	0.9
$\text{ML}_6(\text{CN} = 6)$	1.3
$\text{ML}_7(\text{CN} = 7)$	1.2
NO_3	2.1
N_3	1.3
N_2H_4	0.4
Cl	1.2
Alkyl	0.6

^aM is metal and N is any ligand that contains nitrogen that is bridged between two metals

^bM is metal and L is ligand that is bonded to metal

^cCoordination number of metal

or to choose proper descriptors that improve performance of model, successive rounds of cross-validation, LOO-CV and k-fold CV, should be used.

One single data point is removed as a tester in LOO-CV, while in k-fold CV, the dataset is split into k groups, randomly, and one group is put away as the tester in each run. The procedure of splitting, calibrating, and testing of sub-models is repeated several hundred times in order to control

the flexibility of model and to achieve a stable result for k-fold CV. Finally, Q^2 which is a mean cross-validated R^2 , is derived [27, 28]. Since the R^2 and Q^2 values for new model are greater than 0.6 and 0.5; respectively, the model can be considered as a predictive model [29]. Internal validation was done by using the MATLAB[®] software in this work. Moreover, eight independent MOFs with complicated structure that was not used in the model building were used for external validation.

Results and discussion

Construction of the new model

The study of T_{decom} values of different MOFs revealed that it is possible to construct a new model based on the number of atoms and some structural parameters. It has been cleared that coordination number and coordination environment have more effects than other parameters, such as framework topology, on the thermal stability of MOFs [12]. Moreover, the presence of some metals, organic compounds, and substituents increase or decrease the predicted T_{decom} . For example, azole derivatives and La are increasing factors. On the contrary, alkyl, Ca, and Cu are decreasing factors, Table 2.

Several combinations of atoms and structural parameters have been tested for construction of a new correlation. $(n_{\text{C}} + n_{\text{O}} + n_{\text{H}} + n_{\text{N}})$ or $(n_{\text{C}}, n_{\text{O}}, n_{\text{H}}, n_{\text{N}})$ separately, $(n_{\text{S}}, n_{\text{Cl}}, n_{\text{C} + \text{O}})$ $(n_{\text{N}}, n_{\text{O}}, n_{\text{Cu}}, n_{\text{Cd}}, n_{\text{Cl}})$, and $\frac{\sum m_x}{\text{MW}}$, where m_x is mass of each atom and MW is molecular weight, and many other combinations have been tested. In each step, R^2 and P value were investigated and best combination was selected based on maximum R^2 and minimum P value.

It was cleared that three variables $n_{\text{S}}, n_{\text{C}} + n_{\text{O}}$ and $n_{\text{N}} + n_{\text{H}} + n_{\text{Cl}}$ have more significant roles than other elements by evaluation of statistical parameters. Accordingly, $n_{\text{S}}, n_{\text{C}} + n_{\text{O}} + n_{\text{N}} + n_{\text{H}} + n_{\text{Cl}}$ and some metals, such as Cu, Zn, Zr, La, Pr, Nd, Sm, Co, Ca, Ag, Cd, Ni, Pb, and Ba

Table 3 Statistical parameters of Eq. (1)

Descriptor	Coefficients	SD	P value	Lower bound (95%)	Upper bound (95%)
Intercept	346.3	12.61	8.032×10^{-32}	321.0	371.7
n_S	9.4	18.07	2.477×10^{-8}	83.08	155.7
$n_C + n_O$	893	0.2151	9.811×10^{-12}	1.461	2.325
$n_N + n_H + n_{Cl}$.6133	0.1471	1.207×10^{-4}	- 0.909	- 0.3180
T_{decom}^+	0.9	72.15	3.718×10^{-10}	416.0	705.8
T_{decom}^-	- 40.77	3.896	3.388×10^{-14}	- 48.60	- 32.95

and linkers such as TPTC, ntz, tztr, atrz, bta, en, hdtz, ..., with specific molecular structures was used to construct new model since there is a good relationship between them and decomposition temperature of MOFs. Finally, T_{decom}^+ and T_{decom}^- factors were used to contribute other structural parameters.

The experimental T_{decom} values, Table 1, were used to derive correlation with a good R square, $R^2 = 0.9124$, using MLR method, as follows:

$$T_{decom} = 346.3 + 119.4n_S + 1.893(n_C + n_O) - 0.6133(n_N + n_H + n_{Cl}) + 560.9T_{decom}^+ - 40.77T_{decom}^- \quad (1)$$

where n_S, n_C, n_O, n_N, n_H and n_{Cl} are the number of sulfur, carbon, oxygen, nitrogen, hydrogen, and chlorine atoms in SBUs, respectively; T_{decom}^+ and T_{decom}^- are two correcting factors, that are used to demonstrate increasing and decreasing factors based on further structural parameters, respectively.

The relation between the coordination number and the local coordination environment in SBUs with T_{decom} is shown in Table 2. For example, the values of T_{decom}^+ and T_{decom}^- should be considered for different SBUs in $[Cu(tztr)]_n$ [30] and $[Cu(ntz)]_n$ [31] MOFs. Both MOFs consist of Cu centers, but they have different thermal behavior since the SBUs environment is different. Furthermore, the coordination number of Cu in $[Cu(tztr)]_n$ is not same as $[Cu(ntz)]_n$. In fact both MOFs have a different number of C, O, N, H, and Cl atoms in their structures. Due to the different coordination numbers and different coordination environments, experimental T_{decom} values for $[Cu(tztr)]_n$ and $[Cu(ntz)]_n$ are 360 °C and 315 °C, respectively.

The values of T_{decom}^+ and T_{decom}^- or different coordination numbers and environment in SBUs are shown in Table 2. As seen, some substituents such as triazole, nitrate, chlorine, alkyl, azide, and hydrazine, also some metals such as Ca or La, are important parameters for different values for T_{decom}^+ and T_{decom}^- . Moreover coordination number of metal centers is an important parameter for T_{decom} [3, 12].

Evaluation of the new model by statistical parameters

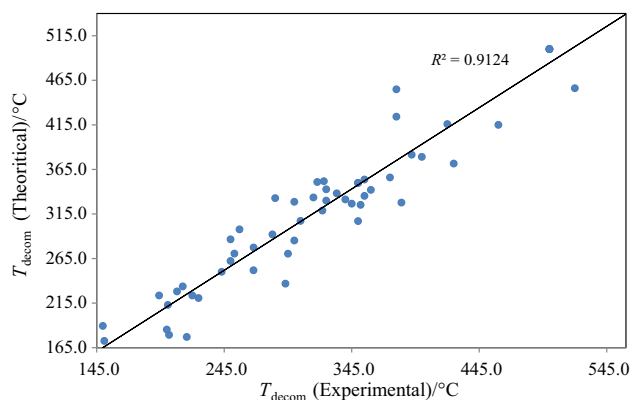
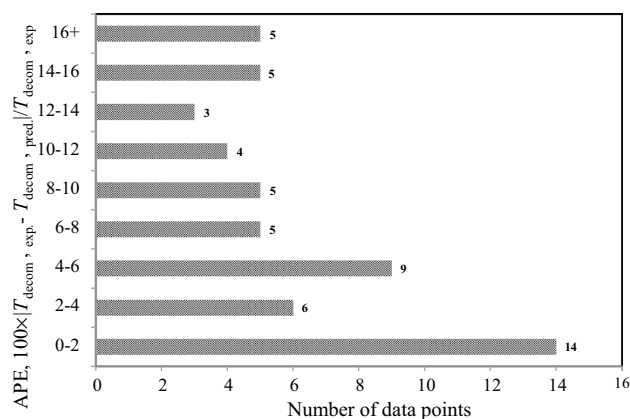
Some statistical parameters related to Eq. (1) such as coefficients, standard deviation, SD, P value, and lower and upper bounds 95% are shown in Table 3. As seen, the value of SD for each descriptor is much smaller than corresponding coefficient, which indicates that the variables are significant. The SD values are useful measures for the precision of estimation of each coefficient and the small standard errors show good precision [32]. The probability value, P value, refers to the probability that, the absolute value would be greater than or equal to the actual observed results [33]. If the P value < 0.05 , it means that null hypothesis is rejected. The null hypothesis is a general statement or default position that there is no relationship between two measured phenomena, or no association among groups [34]. Since the results of P value for all variants in Table 3, are less than 0.05, it confirms that there are significant relationships between the dependent variable and independent variables.

The predicted T_{decom} using new model versus experimental T_{decom} of MOFs given in Table 1 is shown in Fig. 1, and the range of the absolute percent errors of new model for these data is shown in Fig. 2. As seen the predicted values are close to experimental data that indicates the new model has low absolute percent errors.

Cross-validation of new model has been done, and statistical parameters are shown in Table 5. The value of Q^2 refers to goodness of prediction and usually is smaller than R^2 , but in robust models, there are not very huge differences between Q^2 and R^2 [35, 36]. If R^2 is greater than 0.6 and its Q^2 values are greater than 0.5, the model is a proper model [29]. As a result of cross-validation, the coefficient of determination for LOO-CV, Q_{LOO}^2 , of Eq. (1) is 0.8903. Also after 1000 runs, the average for fivefold CV, Q_{5CV}^2 , is 0.8560. It was realized that Eq. (1) is a reliable predictive model since values of important parameters such as R^2 , Q_{LOO}^2 , and Q_{5CV}^2 are significantly greater than the threshold values for R^2 and Q^2 , i.e., 0.6 and

Table 4 The predicted decomposition onset temperatures of MOFs, compared to the experimental values

No.	SBU	Experimental $T_{\text{decom}}/^{\circ}\text{C}$	Predicted $T_{\text{decom}}/^{\circ}\text{C}$	Dev.
1	$[\text{Co}_2(\text{N}_2\text{H}_4)_4(\text{N}_2\text{H}_3\text{CO}_2)_2][\text{ClO}_4]_2 \cdot \text{H}_2\text{O}$	231 [30]	233	- 2
2	$\text{Cr}_3\text{F}(\text{H}_2\text{O})_2\text{O}[(\text{O}_2\text{C})-\text{C}_6\text{H}_4-(\text{CO}_2)]_3$	290 [62]	357	- 67
3	$\text{Cr}_3\text{F}(\text{H}_2\text{O})_2\text{O}[(\text{O}_2\text{C})-\text{C}_6\text{H}_4-(\text{CO}_2)]_3 \text{C}_2\text{H}_3(\text{NH}_2)_2$	350 [62]	331	+19
4	$\text{Cr}_3\text{F}(\text{H}_2\text{O})_2\text{O}[(\text{O}_2\text{C})-\text{C}_6\text{H}_4-(\text{CO}_2)]_3 \text{C}_{10}\text{H}_{15}\text{N}_2\text{O}_8$	350 [62]	356	- 6
5	$[\text{Cu}_3(\text{L}_{(109)}^{6-})(\text{H}_2\text{O})_3]_n$	325 [63]	317	+8
6	$[\text{Cu}_3(\text{L}_{(110)}^{6-})(\text{H}_2\text{O})_3]_n$	325 [63]	322	+3
7	$[\text{Ca}_2(\text{H}_2\text{O})(\text{H}_2\text{gal})_2] \cdot 2\text{H}_2\text{O}$	220 [52]	234	- 14
8	$\{[\text{Zn}(\text{C}_{12}\text{H}_{10}\text{N}_4)_2(\text{SiF}_6)](\text{CH}_2\text{Cl}_2)\}_n$	220 [64]	248	- 28

**Fig. 1** The predicted T_{decom} ($^{\circ}\text{C}$) versus experimental values**Fig. 2** The range of the absolute percent errors of new model

0.5, respectively. Moreover, the cross-validation shows that the new model is robust and well-behaved model since both the Q_{LOO}^2 and $Q_{5\text{CV}}^2$ values are close to the R^2 . Finally, some

Table 5 Statistical parameters in cross-validation for the new model

Parameter	New model	Cross-validation	
		Leave-one-out	Fivefold ^a
Coefficients of determination	0.9124 ^b	0.8903 ^c	0.8560 ^d
MAPE	7.3 ^e	8.1 ^f	8.8 ^g
RMSE	28.1 ^h	31.5 ⁱ	32.3 ^j

^aFor 100 runs

^b R^2

^c Q_{LOO}^2

^d $Q_{5\text{CV}}^2$

^e $\text{MAPE}_{\text{Model}}$

^f MAPE_{LOO}

^g $\text{MAPE}_{5\text{CV}}$

^h $\text{RMSE}_{\text{Model}}$

ⁱ RMSE_{LOO}

^j $\text{RMSE}_{5\text{CV}}$

other statistical parameters such as the mean absolute percent error, MAPE, and root-mean-squared error, RMSE, values for LOO-CV and fivefold CV are measured from cross-validation, that are close to the MAPE and RMSE of Eq. (1).

For assessing the reliability of new model, T_{decom} of eight further MOFs were calculated by Eq. 1. As shown in Table 4, there is no significant deviation between predicted and experimental T_{decom} values that indicate new method has a good reliability. Some statistical parameters for new model and external validation are given in Table 6. As shown, RMSE, MAPE, and max error for eight MOFs are less than new model, which indicates that external validation test for eight further MOFs is proper.

Table 6 External validation for new model

Data set	Data points	RMSE	MAPE	Max Error	R ²	F statistic	Significance F
New model	56	28.1	7.3	74.9	0.9124	104.177	3.22 × 10 ⁻²⁵
External validation	8	27.3	6.7	67	–	–	–

Conclusions

A novel and accurate model was introduced for prediction of T_{decom} of different MOFs. This model is based on the structural parameters and needs the number of $n_S, n_C + n_O, n_N + n_H + n_{Cl}$ and also two correcting factors T_{decom}^+ and T_{decom}^- . Some substituents, metals, and coordination number of metal centers are important parameters for different values for T_{decom}^+ and T_{decom}^- . Through the new model, one can predict the T_{decom} for new designed MOFs using some structural parameters. The reliability of new model was approved by internal and external validations.

References

- Li M, Li D, O’Keeffe M, Omar MY. Topological analysis of metal–organic frameworks with polytopic linkers and or multiple building units and the minimal transitivity principle. *Chem Rev.* 2014;114:1343–70.
- Kim J, Chen B, Reineke TM, Li H, Eddaoudi M, Moler DB, O’Keeffe M, Yaghi OM. Assembly of metal–organic frameworks from large organic and inorganic secondary building units new examples and simplifying principles for complex structures. *J Am Chem Soc.* 2001;123:8239–47.
- Weigang L, Zhangwen W, Zhi-Yuan G, Tian-Fu L, Jinhee P, Jihye P, Jian T, Muwei Zh, Qiang Z, Thomas G, Mathieu B, Hong-Cai Z. Tuning the structure and function of metal–organic frameworks via linker design. *Chem Soc Rev.* 2014;43:5561–93.
- Stock N, Biswas S. Synthesis of metal–organic frameworks (MOFs): routes to various MOF topologies, morphologies, and composites. *Chem Rev.* 2012;112:933–69.
- Eddaoudi M, Kim J, Rosi N, Vodak D, Wachter J, O’Keeffe M, Omar MY. Systematic design of pore size and functionality in isorecticular MOFs and their application in methane storage. *Science.* 2002;295:469–72.
- Yuan S, Feng L, Wang K, Pang J, Bosch M, Lollar C, Sun Y, Qin J, Yang X, Zhang P, Wang Q, Zou L, Zhang Y, Zhang L, Fang Y, Li J, Zhou HC. Stable metal–organic frameworks design, synthesis, and applications. *Adv Mater.* 2018;30:1704303.
- Lee JY, Farha OK, Roberts J, Scheidt KA, Nguyen ST, Hupp JT. Metal–organic framework materials as catalysts. *Chem Soc Rev.* 2009;38:1450–9.
- Qin JS, Zhang JC, Zhang M, Du DY, Li J, Su ZM, Wang YY, Pang SP, Li SH, Lan YQ. A highly energetic N-rich zeolite-like metal–organic framework with excellent air stability and insensitivity. *Adv Sci.* 2015;2:1500150.
- Wu BD, Yang L, Wang SW, Zhang TL, Zhang JG, Zhou ZN, Yu KB. Preparation, crystal structure, thermal decomposition, and explosive properties of a novel energetic compound $[Zn(N_2H_4)_2(N_3)_2]_n$: a new high-nitrogen Mmaterial (N = 65.60%). *Z Anorg Allg Chem.* 2011;637:450–5.
- Bushuyev OS, Peterson GR, Brown P, Maiti A, Gee RH, Weeks BL, Hope-Weeks LJ. Metal–organic frameworks (MOFs) as safer, structurally reinforced energetics. *Chem Eur J.* 2013;19:1706–11.
- Li S, Wang Y, Qi C, Zhao X, Zhang J, Zhang S, Pang S. 3D energetic metal–organic frameworks: synthesis and properties of high energy materials. *Angew Chem Int Ed.* 2013;52:14031–5.
- Mu B, Walton KS. Thermal analysis and heat capacity Sstudy of metal–organic frameworks. *J Phys Chem C.* 2011;115:22748–54.
- Makal TA, Wang X, Zhou HC. Tuning the moisture and thermal stability of metal–organic frameworks through incorporation of pendant hydrophobic groups. *Cryst Growth Des.* 2013;13:4760–8.
- Bosch M, Zhang M, Zhou HC. Increasing the stability of metal–organic frameworks. *Adv Chem.* 2014;2014:1–8.
- Kleist W, Maciejewski M, Baiker A. MOF-5 based mixed-linker metal–organic frameworks: Synthesis, thermal stability and catalytic application. *Thermochim Acta.* 2010;499(1–2):71–8.
- Park KS, Ni Z, Cote AP, Choi JY, Huang R, Uribe-Romo FJ, Chae HK, O’Keeffe M, Yaghi OM. Exceptional chemical and thermal stability of zeolitic imidazolate frameworks. *Proc Natl Acad Sci USA.* 2006;103:10186–91.
- Howarth AJ, Liu Y, Li P, Li P, Wang TC, Hupp JT, Farha OK. Chemical, thermal and mechanical stabilities of metal–organic frameworks. *Nat Rev Mater.* 2016;1:1–15.
- Furukawa H, Cordova KE, O’Keeffe M, Yaghi OM. The chemistry and applications of metal–organic frameworks. *Science.* 2013;341:1230444.
- Kandiah M, Nilsen MH, Usseglio S, Jakobsen S, Olsbye U, Tilset M, Larabi C, Quadrelli EL, Bonino F, Lillerud KP. Synthesis and stability of tagged UiO-66 Zr-MOFs. *Chem Mater.* 2010;22:6632–40.
- Dehmer M, Emmert-Streib F, Graber A, Salvador A. Statistical modelling of molecular descriptors in QSAR/QSPR. Hoboken: Wiley; 2011.
- Fayet G, Rotureau P, Adamo C. On the development of QSPR models for regulatory frameworks: The heat of decomposition of nitroaromatics as a test case. *J Loss Prevent Proc.* 2013;26:1100–5.
- Yu X, Huang L. Prediction of the onset temperature of decomposition of lubricant additives. *J Therm Anal Calorim.* 2017;130:943–7.
- Keshavarz MH, Esmaeilpour K, Saani MH, Taghizadeh H. A new method for assessment of glass transition temperature of ionic liquids from structure of their cations and anions without using any computer codes. *J Therm Anal Calorim.* 2017;130:2369–87.
- Ghani K, Keshavarz MH, Jafari M, Khademian F. A novel method for predicting decomposition onset temperature of cubic polyhedral oligomeric silsesquioxane derivatives. *J Therm Anal Calorim.* 2017;132:761–70.
- Hawkins DM, Basak SC, Mills D. Assessing model fit by cross-validation. *J Chem Inf Comput Sci.* 2003;43:579–86.
- Gramatica P. Principles of QSAR models validation: internal and external. *QSAR Comb Sci.* 2007;26:694–701.
- MacLennan J, Tang ZH, Crivat B. Data mining with microsoft SQL server 2008. New York: Wiley; 2009.
- Golbraikh A, Tropsha A. Beware of Q^2 ! *J Mol Graph Model.* 2002;20:269–76.
- Tropsha A. Best practices for QSAR model development, validation, and exploitation. *Mol Inf.* 2010;29:476–88.

30. Zhang Y, Zhang S, Sun L, Yang Q, Han J, Wei Q, Xie G, Chen S, Gao S. Solvent-free dense energetic metal-organic framework (EMOF): to improve stability and energetic performance via in situ microcalorimetry. *Chem Comm.* 2017;53:3034–7.
31. Qu X, Zhai L, Wang B, Wei Q, Xie G, Chen S, Gao S. Copper-based energetic MOFs with 3-nitro-1H-1,2,4-triazole: solvent-dependent syntheses, structures and energetic performances. *Dalton T.* 2016;45:17304–11.
32. Montgomery DC, Runger GC. *Applied Statistics and Probability for Engineers*. 6th ed. Hoboken: Wiley; 2014.
33. Wasserstein RL, Lazar NA. The ASA's statement on p-values: context, process, and purpose. *Am Stat.* 2016;70:129–33.
34. Everitt BS. *The Cambridge dictionary of statistics*. Institute of Psychiatry, King's College, University of London. 2002;1:1–410.
35. Leach AR, Gillet VG. *An introduction to chemoinformatics*. Springer. 2007;1:1–255.
36. Fayet G, Rotureau P. Development of simple QSPR models for the impact sensitivity of nitramines. *J Loss Prevent Proc.* 2014;30:1–8.
37. Friedrich M, Galvez-Ruiz JC, Klapotke TM, Mayer P, Weber B, Weigand JJBTA. copper complexes. *Inorg Chem.* 2005;44:8044–52.
38. Wu BD, Bi YG, Li FG, Yang L, Zhou ZN, Zhang JG, Zhang TL. A novel stable high-nitrogen energetic compound: Copper(II) 1,2-diaminopropane azide. *Z Anorg Allg Chem.* 2014;640:224–8.
39. Zhang S, Yang Q, Liu X, Qu X, Wei Q, Xie G, Chen S, Gao S. High-energy metal-organic frameworks (HE-MOFs): Synthesis, structure and energetic performance. *Coord Chem Rev.* 2016;307:292–312.
40. Liu X, Gao W, Sun P, Su Z, Chen S, Wei Q, Xie G, Gao S. Environmentally-friendly high-energy MOFs crystal structure, thermostability, insensitivity and remarkable detonation performance. *Green Chem.* 2015;17:831–6.
41. Wang SH, Zheng FK, Wu MF, Liu ZF, Chen J, Guo GC, Wu AQ. Hydrothermal syntheses, crystal structures and physical properties of a new family of energetic coordination polymers with nitrogen-rich ligand N-[2-(1H-tetrazol-5-yl)ethyl]glycine. *CrystEngComm.* 2013;15:2616–23.
42. Feng Y, Liu X, Duan L, Yang Q, Wei Q, Xie G, Chen S, Yang X, Gao S. In situ synthesized 3D heterometallic metal-organic framework (MOF) as a high-energy-density material shows high heat of detonation, good thermostability and insensitivity. *Dalton T.* 2015;44:2333–9.
43. Liu X, Yang Q, Su Z, Chen S, Xie G, Wei Q, Gao S. 3D high-energy-density and low sensitivity materials: synthesis, structure and physicochemical properties of an azide-Cu(II) complex with 3,5-dinitrobenzoic acid. *Rsc Adv.* 2014;4:16087–93.
44. Yongan F, Yangang B, Wenyuan Z, Tonglai Z. anionic metal organic framework lead the way to eco-friendly high energy density material. *J Mater Chem A.* 2016;4:7596–600.
45. Cudzilo S, Nita M. Synthesis and explosive properties of copper(II) chlorate(VII) coordination polymer with 4-amino-1,2,4-triazole bridging ligand. *J Hazard Mater.* 2010;177:146–9.
46. Yalu D, Panpan P, Baoping H, Hui S, Shenghua L, Siping P. High-density energetic metal-organic frameworks based on the 5,5'-Dinitro-2H,2'H-3,3'-bi-1,2,4-triazole. *Molecules.* 2017;22:1068.
47. Orefuwa SA, Yang Y, Goudy AJ. Rapid solvothermal synthesis of an isoreticular metal-organic framework with permanent porosity for hydrogen storage. *Micropor Mesopor Mat.* 2012;153:88–93.
48. Botas JA, Calleja G, Sánchez-Sánchez M, Orcajo MG. Effect of Zn/Co ratio in MOF-74 type materials containing exposed metal sites on their hydrogen adsorption behaviour and on their band gap energy. *Int J Hydrogen Energ.* 2011;36:10834–44.
49. Xie K, Fu Q, He Y, Kim J, Goh SJ, Nam E, Qiao GG, Webley PA. Synthesis of well dispersed polymer grafted metal-organic framework nanoparticles. *Chem Commun.* 2015;51:15566–9.
50. DeCoste JB, Peterson GW, Schindler BJ, Killops KL, Browe MA, Mahle JJ. The effect of water adsorption on the structure of the carboxylate containing metal-organic frameworks Cu-BTC, Mg-MOF-74, and UiO-66. *J Mater Chem A.* 2013;1:11922–32.
51. D'Vries RF, Iglesias M, Snejko N, Alvarez-Garcia S, Gutiérrez-Puebla E, Monge MA. Mixed lanthanide succinate-sulfate 3D MOFs: catalysts in nitroaromatic reduction reactions and emitting materials. *J Mater Chem.* 2012;22:1191–8.
52. Crespo TL. Engineered surface metal organic frameworks (MOFs) for encapsulation and delivery of macromolecules. PhD Thesis, University of Santiago de Compostela. 2015:1–498.
53. Xu CX, Zhang JG, Yin X, Jin X, Li T, Zhang TL, Zhou ZN. Cd(II) complexes with different nuclearity and dimensionality based on 3-hydrazino-4-amino-1,2,4-triazole. *J Solid State Chem.* 2015;226:59–65.
54. Gao W, Liu X, Su Z, Zhang S, Yang Q, Wei Q, Chen S, Xie G, Yang X, Gao S. High-energy-density materials with remarkable thermostability and insensitivity: syntheses, structures and physicochemical properties of Pb(II) compounds with 3-(tetrazol-5-yl) triazole. *J Mater Chem A.* 2014;2:11958–65.
55. Tang Z, Zhang JG, Liu ZH, Zhang TL, Yang L, Qiao XJ. Synthesis, structural characterization and thermal analysis of a high nitrogen-contented cadmium (II) coordination polymer based on 1,5-diaminotetrazole. *J Mol Struct.* 2011;1004:8–12.
56. Xia Z, Chen S, Wei Q, Qiao C. Syntheses and characterization of energetic compounds constructed from alkaline earth metal cations (Sr and Ba) and 1,2-bis(tetrazol-5-yl)ethane. *J Solid State Chem.* 2011;184:1777–83.
57. Liu Z, Zhang T, Zhang J, Wang S. Studies on three-dimensional coordination polymer $[Cd_2(N_2H_4)_2(N_3)_4]_n$: crystal structure, thermal decomposition mechanism and explosive properties. *J Hazard Mater.* 2008;154:832–8.
58. Zhang S, Liu X, Yang Q, Su Z, Gao W, Wei Q, Xie G, Chen S, Gao S. A new strategy for storage and transportation of sensitive high-energy materials: guest-dependent energy and sensitivity of 3D metal-organic-framework-based energetic compounds. *Chem Eur J.* 2014;20:7906–10.
59. Mu B, Huang Y, Walton KS. A metal-organic framework with coordinatively unsaturated metal centers and microporous structure. *CrystEngComm.* 2010;12:2347–9.
60. Mu B. Synthesis and gas adsorption study of porous metal-organic framework materials. PhD thesis, Georgia Institute of Technology. 2011:1–216.
61. Heck R, Bacsá J, Warren JE, Rosseinsky MJ, Bradshaw D. Triply interpenetrated (3,4)- and (3,5)-connected binodal metal-organic networks prepared from 1,3,5-benzenetrisbenzoate and 4,4'-bipyridyl. *CrystEngComm.* 2008;10:1687–92.
62. Bai ZQ, Yuan L, Zhu L, Liu ZR, Chu SQ, Zheng LR, Zhang J, Chai ZF, Shi WQ. Introduction of amino groups into acid-resistant MOFs for enhanced U(VI) sorption. *J Mater Chem A.* 2015;3:525–34.
63. Farha OK, Eryazici I, Jeong NC, Hauser BG, Wilmer CE, Sargeant AA, Snurr RQ, Nguyen ST, Yazaydin AO, Hupp JT. Metal-organic framework materials with ultrahigh surface areas: is the sky the limit? *J Am Chem Soc.* 2012;134:15016–21.
64. Manna B, Sharma S, Ghosh SK. Synthesis and Crystal Structure of a Zn(II)-Based MOF Bearing Neutral N-Donor Linker and SiF_6^{2-} Anion. *Crystals.* 2018;8:37.

Publisher's Note Springer Nature remains neutral with regard to jurisdictional claims in published maps and institutional affiliations.